IJMTST is UGC Approved Journal with Journal Id: 43137

International Journal for Modern Trends in Science and Technology, 8(S05):52-63, 2022

ISSN: 2455-3778 online
DOI: https://doi.org/10.46501/IJMTST08S0510
Available online at: https://www.ijmtst.com/vol8si05.html

Medical Image Enhancement Using Deep Learning

G.V. Vinod | P. Jahir khan | K. Navya Sri | P. Ashok | A. Venkateswara Reddy

Department of Electronics and Communication Engineering, Godavari Institute of Engineering and Technology(A), JNTUK, Kakinada.

To Cite this Article
G.V. Vinod, P. Jahir khan, K. Navya Sri, P. Ashok and A. Venkateswara Reddy. Medical Image Enhancement Using Deep Learning. International Journal for Modern Trends in Science and Technology 2022, 8(S05), pp. 52-63. https://doi.org/10.46501/IJMTST08S0510

Article Info
Received: 26 April 2022; Accepted: 24 May 2022; Published: 30 May 2022.

ABSTRACT

Deep Learning image processing techniques are gaining traction in a variety of fields, including medical imaging. Image classification, segmentation, and denoising are among the most common tasks. The goal of this project is to improve Optical Coherence Tomography imaging of the optic nerve head (OCT). We use numerous state-of-the-art image Super-Resolution (SR) technologies instead of directly applying noise reduction techniques. SR up samples the low-resolution (LR) image to match the size of the high-resolution (HR) image. In terms of image enhancement, the up sampled LR image can be thought of as a low-quality, noisy image, whereas the HR image is the desired enhanced version. We tested a variety of image SR architectures, including super- resolution Convolutional Neural Networks.

Key words:—Deep learning . Convolutional neural network .Medical images . Segmentation . Classification . Detection.

1.INTRODUCTION

Deep Neural Networks (DNN) have seen a lot of success in image processing and analysis in recent years, beating humans in some tasks like image categorization. It was just a matter of time before DNNs made an appearance in the field of medical image processing. Because many existing MRI or CT images are of poor quality, improving medical imaging is a work with a high practical value. Traditional image enhancing approaches rely on histogram equali- sation techniques, which are ineffective with medical images. Recently, the DNN has been employed for image enhancement and MRI scan denoising in several studies.

We concentrate on improving or rather denoising pictures generated by Optical Coherence Tomography in this paper (OCT). OCT has become a popular method for examining optic nerve head tissues and monitoring a variety of eye diseases. However, speckle noise, as well as several other abnormalities, degrade the quality of OCT scans. There are several methods for denoising OCT images, both hardware and software-based. Multi-frame averaging, for example, is a hardware technique that dramatically enhances image quality but requires a considerable scanning time. Many patients experience discomfort and stress as a result of this. Filtering and other numerical algorithms are examples of software-based picture denoising techniques.

In the case of OCT image processing, deep learning has only been used for image segmentation and classification thus far.We are aware of only one previous work on OCT denoising.

The purpose of the OCT image enhancement challenge is to increase the quality of a single OCT scan so that it matches the quality of the OCT device's multi-frame averaged image. This would drastically cut the amount of time it takes to produce a high-quality image, as a multi-frame scan can take up to 3 minutes, whereas a single scan takes only a few seconds. This is a supervised multiple regression job from the standpoint of machine learning, as shown in Fig. 1, where the input is a low quality (LQ) single scan and the output is an enhanced high quality (HQ) image mimicking a multi-frame OCT scan.

Researchers in aim to overcome this problem by adding Gaussian noise to high-resolution multi-frame scans and feeding them into a denoising network based on the popular U-net. Because there is typically a misalignment between single scans and their multi-frame counterparts, this strategy eliminates picture registration issues. However, it overlooks the real speckle noise distribution, which may not be Gaussian and is also dependent on the OCT instrument. Our method is distinct in two respects. To begin, we use the original LQ single scans rather than adding fake noise to the HQ multi-frame scans. This appears to necessitate image registration, which we accomplished with the help of the superb Simple ITK toolbox. Second, instead of using image denoising DNN architectures, we modify various state-of-the-art single image super resolution (SR) networks for our objective. Super-resolution Convolutional Neural Network (SRCNN), very deep Convolutional Network (VDSR), deeply recursive Convolutional Network (DRCN), and enhanced super-resolution Generative Adversarial Network (ESRAN) are some of them (ESRGAN). The next part describes how we employ SR networks for picture improvement and provides some information for each of them. We'll go over the data, the settings of the experiment, and the results we got afterwards.

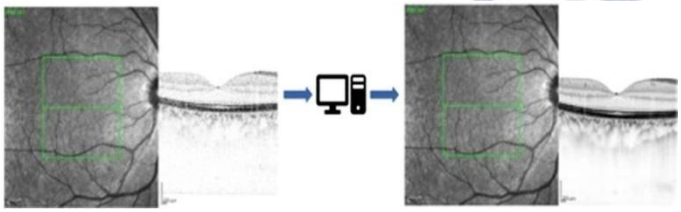

Fig. 1. The task of OCT scan enhancement. Low quality single scans are processed to obtain high quality images resembling the multi-frame scans as closely as possible

Fundamental robotized and human-level basic leadership for tasks ranging from security applications, military missions, and route planning to medicinal diagnostics and business recommender frameworks requires high- quality photographs and recordings. Camera frameworks capture spotless, high-quality photographs that provide better substantiation of an all-around educated method. However, cost constraints prevent large-scale implementation of such frameworks; as a result, suitable sensors are typically used. Inadequate lighting, along with low sensor quality, results in noisy images that could stymie intelligence, surveillance, and reconnaissance (ISR) missions and commercial initiatives.

This project will use 2-dimentional and 3-dimentional deep learning to introduce medical image enhancing technology. For beginners, the essay begins with basic approaches such as convolutional layer, deconvolution layer, loss function, and evaluation functions. Then, employing 2D or 3D convolution neural networks, typical state-of-the-art super-resolution approaches will be presented. Readers can not only compare the network topology but also gain a broad grasp of network performance based on the experimental findings of the network presented in this chapter.

1.1 DEEP LEARNING

Machine learning algorithms have the potential to be profoundly engaged in all sectors of medicine, from drug development to clinical decision making, dramatically transforming how medicine is done. The current success of machine learning algorithms for computer vision tasks comes at a good moment, as medical records are being increasingly digitalized. Between 2007 and 2012, the use of electronic health records (EHR) quadrupled among office-based physicians in the United States, rising from 11.8 percent to 39.6 percent.

Medical images are an important aspect of a patient's electronic health record (EHR) and are currently examined by human radiologists, who are constrained by their speed, weariness, and experience. It takes years and a lot of money to train a trained radiologist, hence some health-care organizations use tele-radiology to

outsource radiology reporting to lower-cost countries like India. The patient suffers from a delayed or incorrect diagnosis. As a result, using an automated, accurate, and efficient machine learning system to do medical image analysis is excellent. Medical image analysis is a hotbed of machine learning research, partially because the data is well-structured and labelled, and it's possible that this will be the first area where patients interact with working artificial intelligence systems.

For two reasons, this is significant. To begin with, medical image analysis is a litmus test for whether artificial intelligence systems would genuinely improve patient outcomes and survival in terms of actual patient metrics. Second, it serves as a testbed for human-AI interaction, determining how amenable patients will be to non-human actors making or assisting them in making health-altering decisions.

When it comes to measuring light, noise is a huge concern. Images are disrupted regardless of how good the sensors are, especially in low-light or gloomy environments. Visual denoising is the process of reducing unwanted image disruption. Image denoising is a technique that takes a noisy image as input and produces a reduced-noise image. Many applications will continue to benefit from advancements in picture enhancement calculations.

Deep learning-based approaches have recently gained a lot of traction after it was discovered that they outperformed other cutting-edge machine learning equipment in a variety of computer vision applications, such as object detection, image classification, and scene interpretation. While neural systems have been extensively studied for picture denoising tasks, no contemporary works employing deep systems to both upgrade and denoise photos captured in ineffectively illuminated settings have been published. We take a representational learning approach to improving low-light photos, using deep auto encoders that can detect basic signals in low-light images and adaptively brighten up and denoise them. The technique takes advantage of adjacent ways to quickly modify complexity, such as the works in, with the purpose of making improvements in relation to neighbours to avoid overcrowding

TYPES OF MEDICAL IMAGING

There are numerous imaging modalities, and their use is becoming more common. From 1996 to 2010, Smith-Bindman et al examined 30.9 million imaging tests across six large integrated healthcare systems in the United States. The scientists discovered that CT, MRI, and PET utilization grew by 7.8%, 10%, and 57%, respectively, across the study period. Ultrasound (US), X-ray, computed tomography (CT) and magnetic resonance imaging (MRI) scans, positron emission tomography (PET) scans, retinal photography, histology slides, and dermo-scopy photographs are all examples of digital medical images. Some of these modalities (such as CT and MRI) assess many organs, whereas others are organ specific (retinal photography, dermo-scopy). Each study's amount of data generated differs as well. A histology slide is a specimen of tissue.

HISTORY OF MEDICAL IMAGE ANALYSIS

The rule-based, expert systems were developed as a result of the symbolic AI paradigm of the 1970s. Short-MYCIN liffe's system, which proposed multiple antibiotic therapy regimens for patients, was one of the first applications in medicine. Parallel to these advancements, AI algorithms transitioned from heuristic-based techniques to manual, handcrafted feature extraction techniques, and finally to supervised learning techniques. Although unsupervised machine learning approaches are being investigated, the majority of the algorithms reported in the literature between 2015 and 2017 used supervised learning methods, such as Convolutional Neural Networks (CNN). Aside from the availability of huge labelled data sets, breakthroughs in GPU hardware have resulted in improved CNN performance and their widespread usage in medical image analysis.

The first artificial neuron was reported by McCulloch and Pitts in 1943, and the perceptron was proposed by Rosenblatt in 1958. An artificial neural network (ANN) is a layer of connected perceptrons that links inputs and outputs, while deep neural networks are numerous layers of ANNs. A deep neural network's advantage is its capacity to learn important low-level features (such as lines or edges) and combine them with higher-level features (such as shapes) in later layer.

This is how the visual cortices of mammals and humans are thought to process visual information and recognize objects. CNNs may have their roots in Fukushima's Neocognitron concept from 1982, but it was Lecun et al. that codified CNNs and employed Rumelhart et alerror .'s backpropagation to successfully conduct the automatic recognition of handwritten digits. After Krizhevsky's work, CNNs became widely used in image recognition. et al. won the 2012 Image-net Large Scale Visual Recognition Challenge (ILSVRC) with a CNN that had a 15% error rate. The runner up had almost double the error rate at 26%. Krizhevsky et al. highlighted key principles used in today's CNNs, such as the usage of Rectified Linear Unit (RELU) functions in CNNs, data augmentation, and dropout. Since then, CNNs have been the most commonly utilized architecture in every ILSVRC competition, even surpassing human performance in image recognition in 2015. As a result, the number of research papers published on CNN design and applications has increased dramatically, making CNNs the dominant architecture in medical image processing.

CONVOLUTIONAL NEURAL NETWORK

To overcome the SR problem, we focus on deep neural network techniques. Dong et al. propose SRCNN as a pioneering technique that learns the mapping from LR to HR pictures in an end-to-end way, outperforming earlier efforts. Later on, network architectures such as a deeper network with residual learning, Laplacian pyramid structure residual blocks, recursive learning, densely connected network, deep back projection, and residual dense network were introduced to the area. Lim et al. offer the EDSR model, which improves significantly by deleting unneeded BN layers in the residual block and enlarging the model size. Zhang et al. recommend that effective residual dense block be used in SR, and they go on to investigate a deeper network with channel attention in order to achieve the best results.

Several approaches for stabilizing the training of a very deep model have been proposed. Residual route, for example, is used to stabilize training and increase performance. Szegedy was the first to use residual scaling, which is also used in EDSR. He et al. offer a stable initialization approach for VGG-style networks without BN for universal deep networks. We create a compact and effective residual-in-residual dense block to assist train a deeper network while also improving perceptual quality.

To increase the visual quality of SR outcomes, perceptual- driven techniques have also been developed. Perceptual loss is a technique for improving visual quality by minimizing error in a feature space rather than pixel space, based on the premise of being closer to perceptual similarity. Contextual loss is a technique for creating photographs with natural image statisticsby focusing on the feature distribution rather than just comparing appearance.

propose an SRGAN model that favours outputs lying on the manifold of natural pictures by using perceptual loss and adversarial loss. design a comparable strategy and investigate the loss of local texture matching Wang et al. propose a spatial feature transform based on these findings to efficiently incorporate semantic prior in an image and improve recovered textures.

Photo-realism is usually achieved through adversarial training with GAN, according to the research. Recently, a number of papers have been published that focus on the development of more effective GAN frameworks. WGAN suggests weight clipping to regularize the discriminator and minimize a reasonable and efficient approximation of the Wasserstein distance. Gradient clipping and spectral normalization are two further better regularization techniques for discriminators. The purpose of the relativistic discriminator is to enhance the chance that created data are real while concurrently lowering the probability that real data are genuine. We improve SRGAN in this paper by using a more effective relativistic average GAN

Several widely used distortion measurements, such as PSNR and SSIM, are commonly used to evaluate SR techniques. These measurements, on the other hand, are fundamentally at odds with human observers' subjective assessments. Perceptual quality is assessed using non-reference measures such as Ma's score and

NIQE, which are both utilized to calculate the perceptual index in the PIRM- SR Challenge. According to a recent study, distortion and perceptual quality are at odds with one another.

The 2-dimensional and 3-dimensional architecture of an organ under investigation are critical in determining what is normal and what is pathological. CNNs are well-suited to conduct image identification tasks because they maintain these local spatial correlations. CNNs have been used for image classification, localization, detection, segmentation, and registration, among other things. Due to its unique feature of keeping local picture interactions while conducting dimensionality reduction, CNNs are the most common machine learning method in image identification and visual learning tasks.

This captures crucial feature relationships inan image (such as how pixels on an edge join to form a line) while also reducing the amount of parameters the algorithm must compute, resulting in increased computational efficiency. CNNs can process both 2-dimensional and 3-dimensional pictures with little alterations as inputs. Because some modalities, such as X-rays, are 2-dimensional, while others, such as CT or MRI scans, are 3-dimensional volumes, this is a useful advantage when creating a system for hospital use.

CNNs and Recurrent Neural Networks (RNNs) are supervised machine learning algorithms that require a lot of training data. Medical image analysis has also been researched using unsupervised learning techniques. Autoencoders, Restricted Boltzmann Machines (RBMs), Deep Belief Networks (DBNs), and Generative Adversarial Networks (GANs) are examples of these (GANs).

2. RELATED WORK

SRCNN is an example of a state-of-the-art deep learning-based SR technique. So, let'shave a look at it and see how it compares to our recommended strategy.

2.1 CONVOLUTIONAL NETWORK FOR IMAGES SUPER RESOLUTION

Model Patch extraction/representation, non-linear mapping, and reconstruction are the three levels of the SRCNN model. Filters with spatial sizes of 9 9, 1 1, and 5 5, respectively, were utilized. After a week of training, we attempted to prepare deeper models but were unable to observe higher performance. In certain circumstances, deeper models outperformed shallower models. They come to the conclusion that deeper networks do not lead to improved performance. However, we believe that increasing depth improves performance greatly. We were able to use 20 weight layers (3-3 for each layer) with success. Our network is extremely dense, and the amount of data used for reconstruction (receptive field) is significantly more (41 41 vs. 13 13).

Training SRCNN directly models high quality images for training. A high-resolution image can be split into low frequency information (which corresponds to a low-resolution image) and high frequency information (which corresponds to a high- resolution image) (residual image or image details). Low- frequency information is shared between the input and output images. This means that SRCNN has two functions: it transports data to the end layer and it reconstructs residuals.

The principle of carrying the input to the end is similar to that of an auto-encoder. It's possible that more training time will be spent learning this auto encoder, lowering the convergence rate of learning the other component (picture details). Because our network directly models the residual pictures, we can achieve considerably faster convergence and even higher accuracy.

Scale SRCNN, like most other SR methods, is trained for a single scale factor and is only expected to work with that scale. As a result, if a new scale is required, a new model must be developed. We need to build unique single scale SR systems for each scale of interest to deal with multiple scale SR (perhaps incorporating fractional factors).

Preparing several individual machines for all potential eventualities in order to cope with different scales, on the other hand, is inefficient and unrealistic. We develop and train a single network to efficiently tackle multiple scale SR problems in this paper. This turns out to be a great solution. For the given sub- task, our single machine outperforms a single-scale expert. We may reduce the number of parameters by three-fold for three scale factors (2, 3, 4).

There are several small changes in addition to the aforementioned concerns. By padding zeros every layer during training, our output image is the same size as the input image, whereas SRCNN output is smaller. Finally, in order to obtain steady convergence, we simply utilize the same learning rates for all layers, whereas SRCNN uses different learning rates for various layers.

3. PROPOSED METHOD

As a fundamental low-level vision problem, single image super-resolution (SISR) has gotten a lot of attention from researchers and AI businesses. The goal of SISR is to recover a high- resolution (HR) image from a single low-resolution (LR) image. Deep convolution neural network (CNN) techniques have flourished since Dong et al. offered the pioneering work ofSRCNN.

SR performance, particularly the Peak Signal-to-Noise Ratio (PSNR) value, has steadily increased thanks to various network architecture designs and training methodologies [5,6,7,1,8,9,10,11,12]. However, because the PSNR metric fundamentally conflicts with human observers' subjective judgement, these PSNR-oriented techniques tend to produce over-smoothed results withinsufficient high-frequency information.

Several perceptual-driven strategies for improving the visual quality of SR results have been presented. Perceptual loss, for example, is proposed to optimize a super- resolution model in feature space rather than pixel space. To encourage the network to select solutions that appear more like natural photos, SR introduces agenerative adversarial network.

The semantic image prior is also used to improve the texture details that are recovered. SRGAN is one of the key milestones on the path to achieving visually acceptable outcomes. In a GAN framework, the basic model is generated with residual blocks and optimized using perceptual loss. SRGAN considerably outperforms PSNR-oriented methods in terms of overall visual quality of reconstruction using all of these techniques.

However, there is still a significant difference between SRGAN results and GT pictures. We revisit the key components of SRGAN in this paper and improve the model in three ways. First, we introduce the Residual-in-Residual Dense Block (RDDB), a higher-capacity and easier-to-train network layout.

To make training a very deep network easier, we remove the Batch Normalization (BN) layers and replace them with residual scaling and smaller initialization. Second, we use Relativistic average GAN (RaGAN) to improve the discriminator. RaGAN learns to determine "if one image is more realistic than the other" rather than "whether one image is real or phoney."

Our tests reveal that this enhancement aids the generator in recovering more realistic texture features. Third, instead of employing the VGG features after activation like in SRGAN, we propose using them before activation to improve perceptual loss. As will be demonstrated, we find that the corrected perceptual loss produces sharper edges and more visually pleasant results.

The perception-distortion plane is divided into three sections, each determined by RMSE thresholds, with the regional champion being the algorithm that obtains the lowest perceptual index in each region. We're concentrating on area 3 because we want to raise perceptual quality tonew heights. Our suggested ESRGAN achieved first place in the PIRM-SR Challenge (region 3) with the best perceptual index thanks to the aforementioned improvements and some other tweaks.

We also offer a network interpolation technique, which can continuously adapt the reconstruction style and smoothness in order to balance visual quality and RMSE/PSNR. Image interpolation, which interpolates images pixel by pixel, is another option. We use this method to compete in both regions 1 and 2. The distinctions between network interpolation and image interpolation algorithms.

4. METHODOLOGY

ENHANCED SUPER RESOLUTION GENERATIVE ADVERSARIAL NETWORK (ESRGAN)

Our primary goal is to increase SR's overall perceptual quality. We first outline our suggested network design in this part, then go into the benefits of the discriminator and perceptual loss. Finally, the network interpolation approach for balancing perceptual quality and PSNR is described.

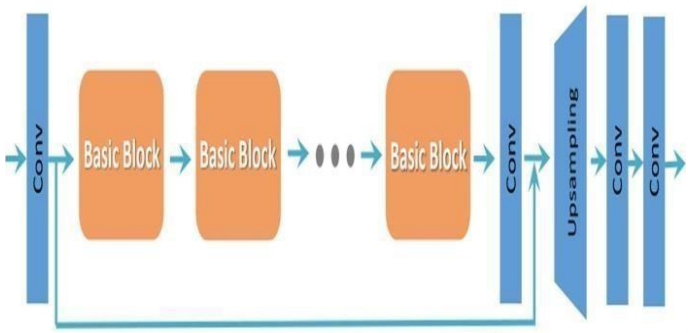

Fig. 2. Block diagram

NETWORK ARCHITECTURE

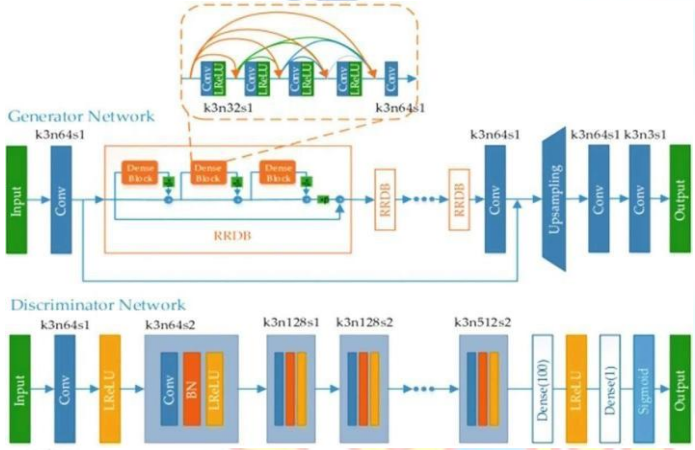

Fig. 3. ESRGAN Architecture

The enhanced super resolution generative adversarial network (ESRGAN) is an improved version of the super resolution generative adversarial network (SRGAN) It is made up of two networks that work together: the Generator and the Discriminator. Figure 3 depicts the structure of each of them. The Generator has several blocks known asresidual in residual dense block (RRDB), which mix multi-level residual networks and dense connections. The Discriminator has a more straightforward construction, with numerous convolution layers followed by batch normalization and Leaky ReLU activation. The Generator uses an upgraded form of the so-called perceptual loss, which distinguishes the ESRGAN from the other SR networks discussed above. The distance between two activated features is minimized on the activation layers of a pre-trained network. As a result, the complete loss of the Generator is given asperceptual loss.

The 1-norm difference between the Generator output G(x) and the target HR picture y, given the input image x. The ESRGAN produces images of higher perceptual quality than the PSNR oriented networks when such loss is used.

PERCEPTUAL LOSS

We also create a more effective perceptual loss L- percep by limiting on characteristics before activation rather than after, as in SRGAN

Johnson et al. suggest perceptual loss, which is expanded in SRGAN, based on the premise of being closer to perceptual similarity. Perceptual loss is defined as the shortest distance between two activated features on the activation layers of a pre-trained deep network.

We suggest, against convention, to employ features before the activation layers, which will address two flaws in the original design. To begin with, the activated features are extremely scarce, particularly after a very deep network. For example, following the VGG19-543 layer, the average percentage of activated neurons for image 'baboon' is only 11.17 percent. Because of the sparse activation, there is insufficient oversight, which leads to poor performance. Second, utilizing features after activation results in inconsistencies in reconstructed brightness when compared to the ground-truth image. Asa result, the generator's total loss is:

$$L_G^{tot} = L_{percep} + \lambda L_G + \eta L_1$$

where L1 = Exi ||G(xi) y||1 is the content loss that determines the 1-norm distance between the recovered image G(xi) and the ground-truth y, and, are the coefficients that balance different loss terms.

In the PIRM-SR Challenge, we also look at a different type of perceptual loss. We design a more suitable perceptual loss for SR – MINC loss – in contrast to the generally used perceptual loss, which uses a VGG network trained for image classification. It's built on a fine-tuned VGG network for material detection that prioritises textures over objects. Despite the fact that the improvement in perceptual index caused by MINC loss is minor, we feel that researching texture-focused perceptual loss is crucial for SR.

NETWORK INTERPOLATION

We offer a flexible and effective strategy network interpolation to eliminate undesirable noise in GAN-based systems while maintaining acceptable perceptual quality. We train a PSNR-oriented network GPSNR initially, and then fine-tune it to get a GAN- based network GGAN. To derive an interpolated model GINTERP, we interpolate all of the appropriate parameters of these two networks.

$$\theta_G^{\mathrm{INTERP}} = (1-\alpha)\,\theta_G^{\mathrm{PSNR}} + \alpha\,\theta_G^{\mathrm{GAN}},$$

GINTERP, GPSNR, and GGAN parameters are INTERP G, PSNR G, and GAN G, respectively, while the interpolation parameter is [0, 1].

There are two advantages to the suggested network interpolation. First, without adding artefacts, the interpolated model can deliver meaningful results for any viable. Second, we can maintain perceptual quality and fidelity without having to retrain the model.

Alternative techniques to balance the effects of PSNR-oriented and GAN-based strategies are also investigated. Instead of using network parameters, one can directly interpolate their output images (pixel by pixel). However, such a technique fails to establish a suitable trade-off between noise and blur, resulting in either too blurry or too noisy with artefacts interpolated images.

Another approach is to adjust the weights of content and adversarial loss, i.e., the parameters and in Eq. However, because this strategy necessitates fine- tuning loss weights and the network, achieving continuous control of the visual style is too expensive.

In order to balance the outcomes of a PSNR-oriented model and a GAN-based technique, we examine the effects of network interpolation and picture interpolation strategies. On both techniques, we use simple linear interpolation. The interpolation parameter is set between 0 and 1 with a 0.2 interval. The pure GAN-based method yields sharper edgesand richer textures, albeit with some undesirable artefacts, whereas the pure PSNR-oriented method yields cartoon-style hazy images.

Unpleasant artefacts are eliminated while textures are preserved via network interpolation. Image interpolation, on the other hand, fails to adequately remove these artefacts. Surprisingly, the network interpolation technique appears to give a smooth adjustment of perceptual quality and fidelity

4. EXPERIMENTS

4.1. PERFOMANCE EVALUATION

The peak noise-to-signal ratio (PSNR) and the structural similarity index measure (SSIM) are two of the most commonly used quantitative performance indicators in image processing. While the authors employed only SNR and SSID metrics, we use PSNR and SSID.

The MSE and PSNR of ground truth picture I and reconstructed image I, both of which have N pixels, are calculated as follows:

$$MSE = \frac{1}{N}\sum_{i=1}^{N}(I(i) - \hat{I}(i))^2$$

$$PSNR = 10\log\left(\frac{L^2}{MSE}\right)$$

where L = 255 for 8-bit pixel encoding. Typical PSNR values vary from 20 to 40, higher is better. On the other hand, the SSID is definedas:

$$SSIM(I,\hat{I}) = \frac{(2\mu_I\mu_{\hat{I}} + C_1)(2\sigma_{I\hat{I}} + C_2)}{(\mu_I^2 + \mu_{\hat{I}}^2 + C_1)(\sigma_I^2 + \sigma_{\hat{I}}^2 + C_2)}$$

where C1 = (k1L)2, C2 = (k2L)2 are constants for avoiding instability, k1<<1, k2<<1 are small constants, and μ and σ2 are the mean and variance of the pixels intensity.

4.1. DATA BASE

We used a limited database of roughly 350 OCT images for the tests. The same targets were utilised for the LQ photos because several of the HQ multi-frame scans had numerous equivalent LQ single scans. The alignment of the majority of the HQ/LQ pairings was necessary, and we used the Simple-ITK image registration toolbox for

this. Six HQ/LQ pairs were chosen for testing, and the rest of the data was divided into 9:1 training and validation sets.

Due to the tiny number of scans, we performed extensive data augmentation, which included horizontal and vertical flips, rotation by many degrees, and other techniques widely employed in image processing. In addition, each scan was cropped into 224 224 non-overlapping sub-images. As a result, we were able to expand the number of training data by a factor of 100.

5. RESULT

This is the largest network in terms of parameters, as well as the number of possible hyper parameters, of all the networks we tested. The RDDB number, the RDB number in each RDDB, the number of convolutional layers, and the number of filters are all critical structurally for the generator. The structure of the discriminator has no significant impact on performance. The RDDB number and the filter number were the most sensitive to the ESRGAN performance in our situation, as shown in Table

1. Because the model was too large to fit in our GPU memory, we were unable to collect results for the situationof RDDB number = 7 and filter number = 16..

TABLE 1: ESRGAN performance in terms of PSNR (dB) and SSIM.

Metric	RDDB number	RDB filter number		
		4	8	16
PSNR	3	19.56	19.01	18.98
	5	19.53	**21.25**	18.92
	7	19.64	18.69	NA
SSIM	3	0.670	0.639	0.725
	5	0.432	0.722	**0.730**
	7	0.658	0.377	NA

In this section, we compare the best PSNR and SSIM results from all of the networks we studied. Figure 8 depicts bar graphs for each metric, as well as the case in which no augmentation is used. In terms of PSNR, the DRCN came out on top, while the SRCNN and VDSR came out on top in terms of SSIM. The acquired metrics values in both situations are significantly better than the baseline, which is the case of unprocessed single scan images.

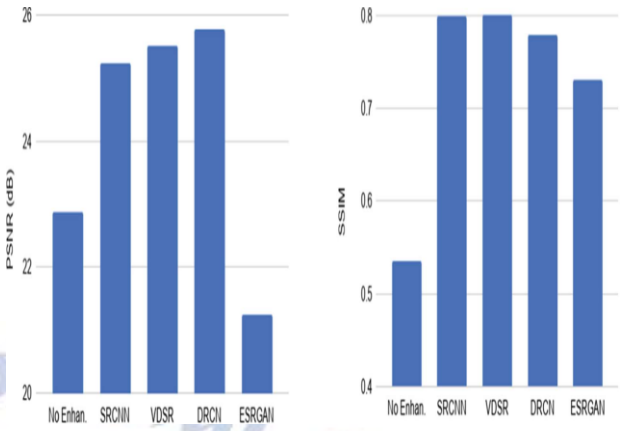

Fig. 4. Comparison of the networks best performances in terms of PSNR and SSIM with thebaseline ("No Enhan.")

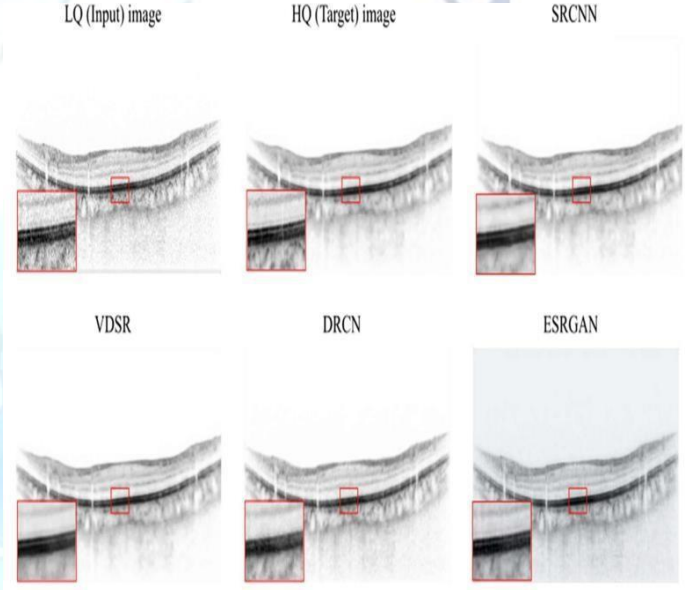

Fig. 5. Example test single scan (first row, left), the corresponding multi-frame averages scan (first row, center), and the results from each network.

6. CONCLUSION

We concentrated on improving single scans generated from Optical Coherence Tomography in this study. They all have speckle noise as well as other artefacts, making it difficult to understand the OCT results. Many OCT devices employ multi-frame averaging techniques to solve this problem, but this takes a long time and causes the patients a lot of discomfort. We used state-of-the-art deep neural networks developed for picture super resolution instead of employing traditional enhancing/denoising methods. Because low-resolution photos are frequently upscaled first, a process that reduces their quality, SR networks basically enhance

those upscaled low-resolution images. We tested many SR networks, including SRCNN, VDSR, DRCN, and ERSGAN, and quantified their performance using PSNR

FUTURE SCOPE

Because they have learned such things during their studies and medical training, the human eye or radiologist may quickly notice the flaws. Similarly, unless you train them by labelling or highlighting the issue and showing it to machine learning algorithms that can identify certain patterns and learn to make the correct forecast, a computer will not be able to find the issue in a medical image annotation.

Conflict of interest statement

Authors declare that they do not have any conflict of interest.

REFERENCES

[1] Y. LeCun, Y. Bengio, and G. Hinton (2015) In-depth research. 436–444 in Nature 521 (7553). https://doi.org/10.1038/nature14539

[2] Razzak MI, Naz ZS, and Zaib A Razzak MI, Naz ZS, and Zaib A (2018) A detailed examination of medical image processing, including an overview, difficulties, and prospects. Self-decision-making is divided into BioApps. 323-350, Springer, Cham, Switzerland. DOI: 10.1007/978-3-319-65981-7 12

[3] S. Pang and X. Yang. Convolutional Extreme Reading Machine and Its Application in Separate Digit Handwriting. 3049632, Hindawi Publ Corp Comput Intell Neurosci 2016. https://doi.org/10.1155/2016/3049632

[4] Chollet, F., et al., Keras, 2015. https://github.com/fchollet.

[5] Zhang Y, Zhang S, and others (2016) Theano: A Python framework for quickly calculating mathematical equations, arXiv prints, abs 1605.02688. http://arxiv.org/abs/1605.02688.

[6] A. Vedaldi, K. Lenc (2015) Matconvnet is a matlab- based convolutional neural network. Procedures for the ACM International Conference, 23rd EditionNeutrosophic sets in the dermoscopic medical imaging category, Guo Y, Ashour A (2019). 229–243 in Neutroscophic Set Med Image Anal 11 (4). 00011-4, https://doi.org/10.1016/B978-0-12-818148-5

[7] R. Merjulah and J. Chandra (2019) Machine learning was used to separate myocardial ischemia into delayed development of comparison. Pages. 209-235 in Intell Data Anal Biomed Appl 10.1016/ B978-0-12-815553- 0.00011-2 https://doi.org/ 10.1016/ B978-0-12-815553- 0.00011-2

[8] Oliveira FPM, Tavares JMRS (2014) A Review of Medical Image Registration. 73-93 in Computer Methods in Biomech and Biomedical Engineering. https://doi.org/10.1080/10255842.2012.670855

[9] Deep FLASH: an effective learning network based on medical picture registration (Wang J, Zhang M, 2020). pp. 4443–4451 in Procedures for the 2020 IEEE / CVF conference on computer vision and pattern recognition (CVPR).2600.2020.00450 https://doi.org/10.1109/cvpr4

[10] Fu, Y., Lei, Y., Wang, T., Curran, W.J., Liu, T., Yang, X. (2020) An in-depth investigation

[11] Abbas A, Abdelsamea MM, Gaber MM; Abbas A, Abdelsamea MM, Gaber MM; Abbas A, Abd (2021) The DeTraC deep convolutional neural network was used to coordinate COVID-19 in chest X-ray pictures. 854–864 in Appl Intell 10.1007/s10489-020-01829-7 https://doi.org/ 10.1007/s10489-020-01829-7

[12] Kowsari K, Sali R, Ehsan L, Adorno W, et al. (2020). Sequential clinical picture design with in-depth learning approach. Information, vol. 11, no. 6, p. 318. https://doi.org/10.3390/info11060318

[13] Singh SP, Wang L, Gupta S, Goli H, Padmanabhan P, Gulyas B, Singh SP, Wang L, Gupta S, Goli H, Padmanabhan P, Gulyas B (2020) A review of an in- depth 3D research of medical imaging. Sensors, vol. 20, no. 18, no. 5097, doi:10.3390/s20185097

[14] Shen D, Wu G, Suk H (2017) An in-depth study on medical image analysis. Annu Rev Biomed Eng 19: 221–248. https://doi.org/10. 1146 / annurev-bioeng-071516-044442

[15] Wang SH, Phillips P, Sui Y, Bin L, Yang M, Cheng H (2018) Alzheimer's disease planning based on an eight-layer neural convolutional network with a modified leaky line unit and extensive integration. J Med Syst 42 (5): 85. https://doi.org/10.1007/ s10916-018-0932-7

[16] Krizhevsky A, Sulskever I, Hinton GE (2012) ImageNet editing with deep convolutional neural networks. Adv Neural Inf Process Syst 60 (6): 84–90. https://doi.org/10.1145/3065386

[17] Szegedy C, Liu W, Jia Y, Sermanet P, Reed S et al (2015) Depth of convolutions. In: Proceedings of the IEEE Computer Society conference on computer vision and pattern recognition; IEEE Computer Society, 7 (12), pp. 1–9

[18] Avants B, Tustison N, Song G (2009) Advanced Orientation Tools (ANTS). Insight.http: //hdl.handle.net/10380/ 3113

[19] Togacar M, Ergen B, Comert Z (2020) The discovery of COVID- 19 using in-depth study models to fully utilize public imitation and formal chest X- ray images using vague color and packaging methods. Elsevier-Comput Biol Med 121: 103805. https: // doi. org / 10.1016 / j.compbiomed.2020.103805

[20] xMinaee S, Kafieh R, Sonka M, Yazdani S, Soufi GJ (2020) Deep-COVID: Predicting COVID-19 in chest X-ray images using in-depth transmission. Elsevier-Med Image Anal 65: 101794.https://doi.org/10.1016/j.media.2020.101794

[21] Apostolopoulos ID, Mpesiana TA (2020) Covid-19: automatic detection of X-ray images used to transfer learning through convolutional neural networks. Springer-Phys Eng Sci Med 43 (2): 635–640. https://doi.org/10.1007/s13246-020-0865-4

[22] Ouchicha C, Ammor O, Meknassi M (2020) CVDNet: an in- depth study novel for the detection of coronavirus (Covid-19) from chest X-ray images. Elsevier-Chaos Solitons Fractals 140 (5): 110245. https://doi.org/10.1016/j.chaos.2020.110245

[23] Sethy PK, Behera SK, Ratha PK (2020) Diagnosis of coronavirus infection (COVID-19) based on deep features and vector support mechanism. Int J Math Eng Manag Sci 5 (4): 643–651. https: // doi. org / 10.33889 / IJMEMS.2020.5.4.052

[24] Jaiswal AK, Tiwari P, Kumar S, Gupta D, Khanna A, Rodrigues JJ (2019) Diagnosis of pneumonia in the chest X-rays: an in- depth study method. Rate 145 (2): 511–518.https://doi.org/10. 1016 / j.measure.2019.05.076

[25] Civit-Masot J, Luna-Perejon F, Dominguez Morales M, Civit A (2020) An in-depth study of assisted diagnosis of COVID-19 using X-ray images of the lungs. Appl Sci 10 (13): 4640. https://doi.org/ 10.3390 / app10134640

[26] Albarqouni S, Baur C, Achilles F, Belagiannis V, Demirci S, Navab N (2016) Aggnet: an in-depth study of the mechanisms of mitosis diagnosis in histological images of breast cancer. IEEE Trans Med Imaging 35: 1313–1321. https://doi.org/10.1109/TMI.2016. 2528120

[27] Anavi Y, Kogan I, Gelbart E, Geva O, Greenspan H (2015) Comparative study of chest radiograph retrieval using binary texts and deep study differences. At: IEEE Engineering Procedures for the Medicine and Biology Society, pages 2940- 2943. https://doi.org/10.1109/EMBC.2015.7319008

[28] Andermatt S, Pezold S, Cattin P (2016) Repetitive units with multi-dimensional gated data fragmentation of biomedical 3D. In: Procedures for in-depth learning in medical image analysis (DLMIA). Computer Science Notes, 10 0 08, pages 142-151

[29] Anthimopoulos M, Christodoulidis S, Ebner L, Christe A, Mougiakakou S (2016) Separation of the lung pattern of interstitial lung disease using a deep convolutional neural network. IEEE Trans Med Imaging 35 (5): 1207– 1216. https://doi.org/10. 1109 / TMI.2016.2535865

[30] Antony J, McGuinness K, Connor NEO, Moran K (2016) Measuring the magnitude of radio graphic osteoarthritis of the knee using deep convolutional neural networks. arxiv: 1609.02469

[31] Apou G, Schaadt NS, Naegel B, Forestier G, Schönmeyer R, Feuerhake F, Wemmert C, Grote A (2016) Acquisition of lobular structures in normal breast tissue. Comput Biol Med 74:91-102https://doi.org/10.1016/j.compbiomed.2016.05.004

[32] Arevalo J, Gonzalez FA, Pollan R, Oliveira JL, Lopez MAG (2016) A study on the representation of mammography mass lesion classification with convolutional neural networks. Computer Systems Biomed Programs127:248257.https://doi.org/10.1016/j. cmpb.2015.12.014

[33] Baumgartner CF, Kamnitsas K, Matthew J, Smith S, Kainz B, Rueckert D (2016) Detection of normal-time aircraft scanning and location detection on fetal ultrasound using fully convolutional neural networks. In: Computer image imaging procedures and computer-assistedinterventions.ComputerScienceNotes,9901,page s 203211.https://doi.org/10.1007/978-3-319- 46723-8_24

[34] Balasamy K, Ramakrishnan S (2019) A smart reverse watermarking system for validating medical images using wavelet and PSO. Clust Comput 22 (2): 4431– 4442. https: // doi. org / 10.1007 / s10586-018-1991-8

[35] Bengio Y (2012) Practical recommendations for gradient-based training for deep structures. Neural Networks: trading strategies. Lesson Notes in Computer Science, 7700, Springer, Berlin, Heidelberg. https://doi.org/10.1007/978-3-642-35289- 8_26

[36] Bengio Y, Courville A, Vincent P (2013) Representing reading: reviews and new ideas. IEEE Trans Pattern Anal Match Intell 35 (8): 1798–1828. https://doi.org/10.1109/TPAMI. 2013.50

[37] Bengio Y, Lamblin P, Popovici D, Larochelle H (2007) Greedy training for deep network frameworks. In: Developmental processes in neural information processing systems, pp 153- 160

[38] Bengio Y, Simard P, Frasconi P (1994) Studying long-term dependence on gradient decline is difficult. IEEE Trans Neu-ral Networks 5 (2): 157–166. https://doi.org/10.1109/72.279181

[39] Benou A, Veksler R, Friedman A, Raviv TR (2016) Comparison interpretation has improved MRI sequences through the integration of deep neural networks. In: Procedures for in- depth learning in medical image analysis (DLMIA). Computer Science Notes, 10 0 08, pages 95- 110. https://doi.org/10.1146/annurev-bioeng-071516-044442

[40] BenTaieb A, Hamarneh G (2016) Topology is fully aware of communication networks through the classification of histology gland. In: Computer image imaging procedures and computer-assisted interventions. Lesson Notes in Computer Science, 9901, pp 460-468. https://doi.org/10.1007/978-3-319-46723-8_53

[41] Silver D, Huang A, Maddison C et al (2016) Becoming an expert in Go game with deep neural networks and tree search. Nature 529:484– 489. https://doi.org/10.1038/nature16961

[42] Mnih V et al (2015) Individual level control by in-depth reinforcement learning. Nature 518:529–533. https://doi.org/10. 1038 / nature14236

[43] Abràmoff MD, Lou Y, Erginay A, Clarida W, Amelon R, Folk JC, Niemeijer M (2016) Advanced automatic detection of diabetic retinopathy in a publicly available database by integrating in-depth study. Plant Ophthalmol Vis Sci 57 (13): 5200–5206. https://doi.org/10.1167/iovs.16- 19964

[44] Akram SU, Kannala J, Eklund L, Heikkila J (2016) network of cell division suggestion to analyze microscopy image. In: Procedures for In- depth Learning in Clinical Diagnostic Analysis (DLMIA). Computer Science Notes, 10 0 08, pp 21-29. https://doi.org/10.1007/978-3-319- 46976-8_3

[45] Ballin A, Karlinsky L, Alpert S, Hasoul S, Ari R, Barkan E (2016) Regional-based convolutional network for tumor detection and classification of breast mammography. In: Procedures for in-depth learning in medical image analysis (DLMIA). Lesson Notes in Computer Science, 10 0 08, pp 197-205. https: // doi.org/10.1007/978-3-319-46976- 8_21

[46] Alansary A et al (2016) The rapid complete automatic separation of the human placenta from the movement of a malformed MRI. In: Computer image imaging procedures and computer-assisted interventions. Computer Science Notes, 9901, pages 589-597. https://doi.org/10.1007/978-3- 319- 46723-8_68

[47] Bergstra J, Bengio Y (2012) Random search for advanced parameter development. J Mach Read Res 13 (10): 281–305

[48] Birenbaum A, Greenspan H (2016) Separation of Longitudinal multiple sclerosis lesions using convolutional neural networks with multiple views. In: Procedures for in-depth learning in clinical image analysis (DLMIA). Computer Science Notes, 10 0 08, pages 58-67. https://doi.org/10.1007/978-3- 319-46976- 8_7

[49] Cheng X, Zhang L, Zheng Y (2015) Studying the deeper similarities of mixed medical images. Computer Methods Biomech Biomed Eng pp248-252. https://doi.org/10.1080/21681163.2015.11352 99

[50] Cicero M, Bilbily A, Colak E, Dowdell T, Gray B, Perampaladas K, Barfett J (2017) Training and validating a deep convolutional network for computer- assisted access and separation of abnormalities on the chest chest radiographs. Plant Radiol 52 (5): 281–287. https://doi.org/10.1097/RLI.0000000000000341

[51] Ertosun MG, Rubin DL Automatic Grading of Gliomas is used for in-depth study of digital pathology images: a modular approach with integration of convolutional neural networks. In: AMIA Annual Series Procedures, pp 1899-908

[52] Balasamy K, Suganyadevi S (2021) Blurred ROI selection of encryption and marking on a medical image using DWT and SVD. Multimedia Tools Appl 80: 7167– 7186. https://doi.org/ 10.1007/ s11042-020- 099815.

[53] Lekadir K, Galimzianova A, Betriu A, Vila MDM, Igual L, Rubin, DL, Fernandez E, Radeva P, Napel S (2017) Convo- lutional neural network for automatic characterization of plaque composition in carotid ultrasound. IEEE J Biomed Health Inform 21 (1): 48– 55. https://doi.org/10.1109/JBHI.2016.2631401

[54] Li R, Zhang W, Suk HI, Wang L, Li J, Shen D, Ji S (2014) Completion of imaging data based on in-depth study to diagnose disease improved brain. Med Image Comput-Assist Interv 17 (Pt 3): 305–312. https://doi.org/10.1007/978-3-319-0443- 0_39

[55] Li W, Manivannan S, Akbar S, Zhang J, Trucco E, McKenna SJ (2016) Separation of glands in colon histology images using handmade features and convolutional neural networks. In: Procedures for international IEEE series of biomedical imaging, pp 1405–1408. https://doi.org/10.1109/ISBI.2016. 7493530

[56] Miao S, Wang ZJ, Liao R (2016) CNN retrieval method for real-time 2D / 3D registration. IEEE Trans Med Imaging 35 (5): 1352– 1363. https://doi.org/10.1109/TMI.2016.2521800

[57] Moeskops P, Viergever MA, Mendrik AM, Vries LSD, Benders MJNL, Isgum I (2016) Automatic classification of MR brain images with a convolutional neural network. IEEE Trans Med Imaging 35 (5): 1252–1262. https://doi.org/10.1109/TMI.2016.2548501

[58] Pinaya WHL, Gadelha A, Doyle OM, Noto C, Zugman A, Cordeiro Q, Jackowski AP, Bressan RA, Sato JR (2016) Using modeling a deep-seated network to distinguish brain morphometry from schizophrenia.NatSciRep6:38897.https://doi.org/10.1038/ srep38897

[59] Plis SM, Hjelm DR, Salakhutdinov R, Allen EA, Bockholt HJ, Long JD, Johnson HJ, Paulsen JS, Turner JA, Calhoun VD (2014) An in-depth study of neuroimaging: a validated study. Former Neurosci 8: 229. https://doi.org/10.3389/fnins.2014. 00229

[60] Poudel RPK, Lamata P, Montana G (2016) Fully convolutional neural networks for multi-slice segmentation of cardiac MRI. arxiv: 1608.03974

[61] Prasoon A, Petersen K, Igel C, Lauze F, Dam E, Nielsen M (2013) A study of the deep aspect of knee cartilage separation using the trilanar convolutional neural network. In: Computer image imaging procedures and computer-assisted interventions. Computer Science Notes, 8150, pages 246-253.https://doi.org/10.1007/978-3-642-40763-5_31

[62] Rajkomar A, Lingam S, Taylor AG, Blum M, Mongan J (2017) Advanced arranging radiographs using deep convolutional neural networks. J Digit Figure 30: 95–101. https: // doi. org / 10.1007 / s10278-016-9914-9

[63] Ravi D, Wong C, Deligianni F, Berthelot M, Andreu Perez J, Lo B, Yang GZ (2017) An in-depth study of health informatics. IEEE J BiomedHealthInform21(1):4–21.https://doi.org/10.1109/JBHI. 2016.2636665

[64] Ravishankar H, Prabhu SM, Vaidya V, Singhal N (2016) Hybrid method for automatic separation of the fetal abdomen from ultrasound images using in-depth study. In: Procedures for IEEE international series on biomedicalimaging,pp.779–78https://doi.org/10.1109/ISBI.2016.749 3382

[65] Samala RK, Chan HP, Hadjiiski LM, Cha K, Helvie MA (2016) Deep- learning convolution neural network of computer- assisted microcalcifications in digital breast tomosynthesis. In: Proceedings 9785, medical imaging, computer-assisted diagnostics, 97850Y. https://doi.org/10.1117/12.2217092

[66] Samala RK, Chan HP, Hadjiiski L, Helvie MA, Wei J, Cha K (2016) Bulk acquisition in digital breast tomosynthesis: a deep network of convolutional neural and transfer learning from mammog- raphy. Med Phys 43 (12): 6654.https://doi.org/10.1118/1.49673 45.

[67] Sarraf S, Tofighi G (2016) Alzheimer's disease planning using fMRI data and in-depth study of convolutional neural networks. arxiv: 1603.08631

[68] Schaumberg AJ, Rubin MA, Fuchs TJ (2016) An in-depth study of H&E slides predicts SPOP status variation in prostate cancer. arxiv: 064279. https://doi.org/10.1101/064279

[69] Suganyadevi S, Shamia D, Balasamy K (2021) IoT-based diet monitoring program for women. Smart Healthc Syst Des Secur Priv Asp. https://doi.org/10.1002/9781119792253.ch8

[70] Spampinato C, Palazzo S, Giordano D, Aldinucci M, Leonardi R (2016) An in-depth study of automated skeletal bone age tests on X-ray images. Med Image Anal 36: 41–51https://doi.org/10. 1016 / j.media

[71] Balasamy K, Shamia D (2021) The skin-based medical marking feature uses a medium-based filter. IETE J Res 1–9. https://doi.org/10.1080/03772063.2021.1893231

[72] Stern D, Payer C, Lepetit V, Urschler M (2016) Automatic age measurement from manual MRI volume using in-depth reading. In: Computer image imaging procedures and computer-assisted interventions. Lesson Notes in Computer Science, 9901, pp 194-202.https://doi.org/10.1007/978-3- 319-46723- 8_23

[73] Suk HI, Shen D (2013) An element based on in-depth learning to represent AD / MCI classification. In: Computer image imaging procedures and computer-assisted interventions. Computer Science Notes, 8150, pp 583– 590.https: //doi.org/ 10.1007 / 978-3-642-40763-5_72

[74] Sun W, Seng B, Zhang J, Qian W (2016) Improving the deep convolutional neural network system for breast cancer diagnosis with unwritten data. Comput Med Imaging Gr 57: 4– 9.https: //doi.org/ 10.1016/ j.compmedimag

[75] Sun W, Zheng B, Qian W (2016) Computer-assisted lung cancer diagnostics with in-depth learning algorithms. In: SPIE medical imaging procedures, 9785, 97850Z. https://doi.org/10.1117/ 12.2216307

[76] Teikari P, Santos M, Poon C, Hynynen K (2016) In-depth tutorial networks for multiphoton microscopy segmentation vasculature. arxiv: 1606.02382

[77] Tran PV (2016) A fully neural convolutional network for cardiac segmentation on MRI of the short axis. arxiv: 1604.00494. abs / 1604.00494